Journal of Applied Microbiology

Journal of Applied Microbiology ISSN 1364-5072

ORIGINAL ARTICLE

Two-dimensional proteome reference map of *Vibrio tapetis*, the aetiological agent of brown ring disease in clams

J. Bermúdez-Crespo[1], S. Balboa[2], J. Alonso[3] and J.L. Romalde[2]

1 Departamento de Genética, Universidad de Santiago de Compostela, Santiago de Compostela, Spain
2 Departamento de Microbiología y Parasitología, CIBUS-Facultad de Biología, Universidad de Santiago de Compostela, Santiago de Compostela, Spain
3 Servicio de Proteómica, Fundación IDICHUS, Hospital Clínico Universitario, Santiago de Compostela, Spain

Keywords
de novo sequencing, MALDI-TOFF, proteome, reference map, *Vibrio tapetis*.

Correspondence
Jesús L. Romalde, Departamento de Microbiología y Parasitología, CIBUS-Facultad de Biología, Universidad de Santiago de Compostela, Campus Vida s/n. 15782, Santiago de Compostela, Spain. E-mail: jesus.romalde@usc.es

2011/2115: received 14 December 2011, revised 14 February 2012 and accepted 21 February 2012

doi:10.1111/j.1365-2672.2012.05271.x

Abstract

Aims: *Vibrio tapetis* is the etiological agent of brown ring disease (BRD) in clams, one of the most threatening diseases affecting this commercially important bivalve. In this study we have constructed a proteome reference map of the *V. tapetis* type strain CECT 4600^T.

Methods and Results: Eighty-two proteins, consistently present in all 2D-gels, were identified by mass spectrometry or by *de novo* sequencing. The majority of the proteins identified (66%) belonged to four COG categories: 'Carbohydrate transport and metabolism', 'Post-translational modification, protein turnover and chaperones', 'Energy production', and 'Amino acid transport and metabolism'. Glyceraldehyde-3-phosphate dehydrogenase, enolase, fructose-bisphosphate aldolase, phosphoglycerate kinase. molecular chaperones Dnak and GroEL, alkyl hydroperoxide reductase, peptidyl-prolyl cis-trans isomerase B and factor Tu, were identified among the 20 most abundant proteins. A comparison of this reference map with that obtained for the *V. tapetis* strain GR0202RD, with different origin and pathophysiological characteristics, was performed.

Conclusions: Under the culture conditions employed in this study, glucose degradation is one of the major pathways for energy production in *Vibrio tapetis*. In addition, the two strains studied, although with remarkable differences at genetic and pathophysiological levels, showed a high similarity under laboratory conditions.

Significance and Impact of the Study: The results obtained here can be considered as a first step to gather valuable information on protein expression, related not only to diverse cellular functions and regulation but also to pathogenesis and bacterium-host interactions in the disease process.

Introduction

Brown ring disease (BRD), caused by *Vibrio tapetis* (Borrego *et al.* 1996), is an epizootic infection described in adult clams. The main sign characterizing the disease is a brown conchiolin deposit on the inner surface of the valves, typically located between the pallial line and the edge of the shell. This organic deposit perturbs the calcification process (Paillard 2004; Paillard *et al.* 1994; Trinkler *et al.* 2010, 2011), causing severe deformations of the clam's shell and subsequently a systemic infection that provokes the death of the animal. Three groups have been described within *V. tapetis*, on the basis of the phenotypic, antigenic and genotypic characteristics of the isolates that correlate with the host origin (Castro *et al.* 1996, 1997; Le Chevalier *et al.* 2003; Rodríguez *et al.* 2006; Romalde *et al.* 2002).

The pathogenicity process is not well established, although it has described that not all *V. tapetis* strains have the same capacity of producing BRD signs and/or mortalities (Novoa *et al.* 1998; Choquet 2004; Paillard 2004). In general, *V. tapetis* shows adhesion capability

towards the clam haemocytes and mantle cells (López-Cortés *et al.* 1999), and an *in vitro* experiment has demonstrated that the cytotoxic effect on clam haemocytes results in cell rounding and the loss of filopods (Lane and Birkbeck 2000; Choquet *et al.* 2003).

Some adherence factors, such as pili, have been identified, and it is known that they allow the colonization and proliferation of this pathogen in the peripheral compartment (Paillard and Maes 1995; Paillard 2004). Haemolysin and exo-enzymes, such as esterase or chymotrypsin, have been detected as extracellular products with a role in pathogenesis (Borrego *et al.* 1996; Allam *et al.* 2001, 2002; Allam and Ford 2006). More recently, it was demonstrated that DjlA (DnaJ-like protein A), an inner membrane-anchored bacterial cochaperone, is involved in *V. tapetis* cytotoxicity (Lakhal *et al.* 2008), as a DjlA defective mutant showed marked reduction in cytotoxicity activity, compared with the wild-type strain, against *Ruditapes philippinarum* haemocytes *in vitro*.

The description of a proteomic reference map can provide valuable data for the protein expression, related to diverse cellular functions and regulation (Phillips and Bogyo 2005; Cash 2009; Cash and Argo 2009), the pathogenesis pathways and the bacterium–host interactions in the disease process (Osman *et al.* 2009; Bumann 2010), as well as the response of a given organism to various external stimuli (Jones *et al.* 2008; Poobalane *et al.* 2008; Roncada *et al.* 2009; Sharma *et al.* 2010). In the last years, the proteomes of some vibrios have been analysed, and several proteins possibly linked to pathogenesis have been characterized (Coelho *et al.* 2004; Kan *et al.* 2004; Lee *et al.* 2006). The knowledge of such reference map is even more important in the case of pathogens such as *V. tapetis,* in which the complete genome was not yet published. This study represents the first description of the reference map of *V. tapetis*.

Material and Methods

Bacterial strains

The type strain CECT 4600^{T} of *Vibrio tapetis,* obtained from Manila clam (*Ruditapes philippinarum*), as well as strain GR0202RD isolated from carpet-shell clam (*Ruditapes decussatus*) in Spain, showing different physiological and genetic characteristics and virulence capacity, were used in this study (Borrego *et al.* 1996; Novoa *et al.* 1998; *Rodríguez et al.* 2006). The bacteria were routinely grown on marine agar (MA) (Pronadisa, Spain) under aerobic conditions at 15°C for 72 h. Stock cultures were maintained frozen at −80°C in marine broth (MB) (Pronadisa, Spain) supplemented with 15% glycerol (v/v).

2DE-PAGE

Growth conditions.
Bacterial inocula were prepared resuspending each strain to achieve 10^9 cells per millilitre adjusting the bacterial suspension to an OD = 1 (508 nm), using a Lambda2 UV/VIS spectrophotometer (Perkin Elmer, Überlinger, Germany).

One flask per strain containing 1 l of sterile MB (Pronadisa, Spain) was inoculated with 250 μl of a 10^8 cells ml^{-1} tube achieving a final concentration of 10^5 cells ml^{-1} and aerobically incubated in a Innova 4340 rotary shaker (70 rev min^{-1}) (New Brunswick Scientific, Edison, NJ, USA) at 15°C for 72 h.

Sample preparation for 2DE-PAGE.
Bacteria were harvested and washed with Tris-buffered sucrose (10 mmol Tris and 250 mmol sucrose pH 7) and lyophilised. Proteins were extracted by suspending 40 mg of lyophilised bacteria in 1 ml standard lysis buffer (7 mol l^{-1} urea, 2 mol l^{-1} thiourea, 4% CHAPS (3-[(3-cholamidopropyl) dimethylammonio]-1-propanesulphonate) and 65 mmol l^{-1} Dithiothreitol (DTT) during 3 h at 27°C. In the middle of digestion, samples were sonicated with three cycles of ten pulses with 15 s of separation between each cycle. Next, samples were centrifuged at 14 000 rpm for 30 min. The resulting supernatants were collected and subjected to protein precipitation using the clean-up kit (GE Healthcare, Piscataway, NJ, USA). After pellet resuspension in other 1 ml of lysis buffer, protein concentration was measured using CB-X protein assay kit (Gbiosciences, Maryland Heights, MO, USA). Finally, the samples were stored at −80°C prior to use.

First dimension.
Isoelectrofocusing (IEF) was performed using a Protean IEF cell (Bio-Rad, Hercules, CA, USA) and 24 cm pH 4–7 IPG strips (GE Healthcare, Uppsala, Sweden). Each 60 μl sample (containing approximately 400 μg of protein) was mixed with 390 μl of rehydration buffer (7 mol l^{-1} urea, 2 mol l^{-1} thiourea, 4% CHAPS, 0·6% DTT, 1% IPG buffer 4–7 and bromophenol blue traces) and loaded in each strip by in-gel rehydration (18). IEF was carried out at 20°C and according to the following steps: active rehydration (50 V) for 12 h, 250 V for 30 min, 500 V for 1 h, 1000 V for 1 h, 4000 V for 2 h, 8000 V for 2 h and 10 000 V to achieve 65 kVh. After IEF, the strips were stored at −20°C until used in second dimension.

Second dimension.
Prior to run the second dimension, the strips were equilibrated at room temperature in equilibration solution (6 mol l^{-1} urea, 50 mmol l^{-1} Tris–HCl pH 8·8, 30%

glycerol and 2% SDS) with the addition of 1% DTT for 15 min, followed by the same solution with the addition of 2·5% of iodoacetamide other 15 min. Strips were fixed with sealed solution (25 mmol l^{-1} Tris, 192 mmol l^{-1} glycine, 0·1% SDS, 0·5% agarose and 0·01% bromophenol blue) on top of a 21 × 26 cm 12,5% polyacrylamide gel. Second dimension was performed according to Laemmli (Laemmli 1970), in a EttanDalt-Six (GE Healthcare) at 30°C overnight (5 mA/gel for 1 h, 10 mA/per 1 h, followed by 16 mA/gel until bromophenol blue dye reached the bottom of the gel).

Two independent cultures as well as three replicates gel per culture were performed to assess the reproducibility of the experiment.

Protein visualization and analysis.
Gels were stained with Coomassie Brilliant Blue (CBB). CBB staining was carried out according to Neuhoff's protocol with minor modifications (Neuhoff *et al.* 1988). Gels were fixed in 50% ethanol, 3% phosphoric acid for 3 h and then washed in H_2O three times for 20 min each. The gels were preincubated in 34% methanol, 17% sulphate ammonium and 3% phosphoric acid for 1 h. Next, 0·35 g l^{-1} of Coomassie Blue G-250 (Bio-Rad) was added to this solution. Each gel was stained alone in a plastic box with 330 ml of this solution during four days to reach the maximum intensity of staining. Finally, gels were washed in H_2O twice for 25 min each and scanned in a densitometer at 300 dpi resolution. Digitalised images were saved in TIFF format, and gels were stored in vacuum-sealed plastic bags at 4°C. PDQuest Advance software version 8·0 (Bio-Rad) were used for spot detection, spot quantitation and reproducibility study.

Mass spectrometric analysis

Protein features chosen for mass spectrometric analysis were excised from the gels and manually digested as previously described (De La Fuente *et al.* 2011). Dried samples were dissolved in 4 μl of 0·5% HCOOH. Equal volumes (0·5 μl) of peptide and matrix solution, consisted of 3 mg CHCA dissolved in 1 ml of 50% acetonitrile in 0·1% TFA, were deposited using the thin layer method, onto a 384 Opti-TOF MALDI plate (Applied Biosystems, Madrid, Spain). Mass spectrometric data were obtained in an automated analysis loop using 4800 MALDI-TOF/TOF analyzer (Applied Biosystems). MS spectra were acquired in reflectron positive-ion mode with a Nd/YAG, 355-nm wavelength laser, averaging 1000 laser shots, and at least three trypsin autolysis peaks were used as internal calibration. All MSMS (tandem mass spectrophotometry) spectra were performed by selecting the precursors with a relative resolution of 300 (full wide at half maximum, FWHM) and metastable suppression. Automated analysis of mass data was achieved using the 4000 Series Explorer Software V3.5. MS and MSMS spectra data were combined through the GPS Explorer Software v3.6 using Mascot software v2.1. (Matrix Science Ltd, London, UK) to search against a nonidentical protein database (NCBInr release data 20100526), with 30-ppm precursor tolerance, 0·35-Da MSMS fragment tolerance, carbamidomethyl cysteine (CAM) as fixed modification, oxidized methionine as variable modification and allowing one missed cleavage. All spectra and database results were manually inspected in detail using the previous software. Protein scores >56 were accepted as significant ($P < 0·05$), considering positive the identification when protein score CI% (confidence interval) was above 98. In the case of MSMS spectra, total ion score CI% was above 95. Spots not identified with Mascot search engine in the automatic loop were submitted to de novo sequencing. A maximum of eight peptides were launched combining all spectra, allowing a mass tolerance of 0·2 Da and PAM30MS as scoring matrix (4).

Results

Three replicates of the proteome of two independent cultures of *Vibrio tapetis* CECT 4600^T strain were separate on large 2-DE gels in p*I* range of 4–7. Gels within each culture as well as between both cultures showed high reproducibility (Fig. 1). Automatic software analysis was used to determine the spot number in each gel. While total amount of protein loaded on each gel was the same, approximately 400 μg, there was significant variation in spot number between both cultures. Thus, average number (±SD) of spot detected was 428 (±7) and 504 (±9) for first and second culture, respectively. Most of the proteins detected were localised in the acidic part of the pH range studied (Figs 1 and 2). Visual inspection also revealed different protein expression according to different molecular mass region. Thus, most abundant proteins were localised, very close, in high molecular weight region, whereas faintest proteins were localised, more expanded, in low molecular weight region (Figs 1 and 2).

From all visualised proteins, 82 proteins that were consistently present in all gels were identified using mass spectrometry (Fig. 2). Sixty-nine of these 82 proteins were satisfactorily identified using MS or MS/MS, representing 61 different unique proteins (Tables 1 and S1). More than one identification per spot was only obtained for one spot (spot 25) (Table 1). Unidentified proteins (13 proteins) were subjected to *de novo* sequencing to obtain information about their identity (Tables 2 and S2). Identified proteins were classified according to their biological functions using the NCBI COG database (http://

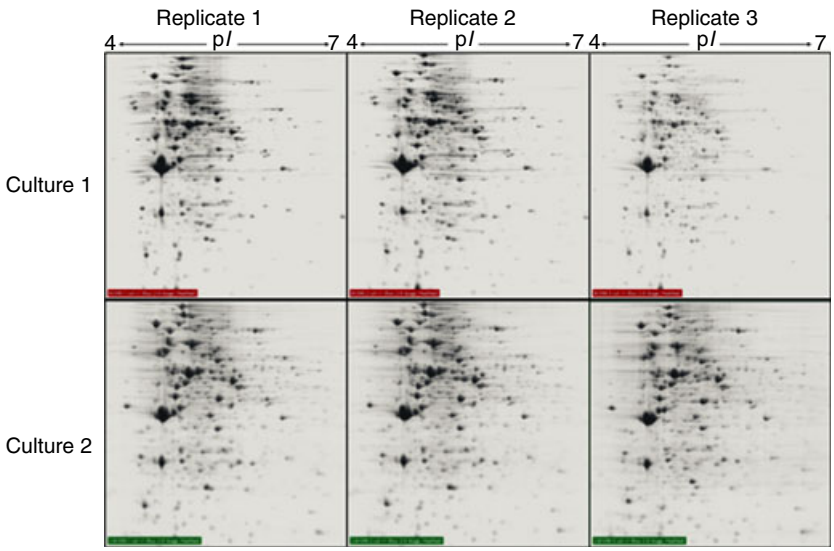

Figure 1 Comparison of 2-DE patterns of the citoplasmic proteins in two cultures of *Vibrio tapetis* CECT 4600^T. IEF was carried out using IPG strips (24 cm, pH 4-7). A 12,5% SDS gel stained with Coomassie G-250 was used in the second dimension. Three replicate gels of each culture were made to assess inter- and intra-variability of the method.

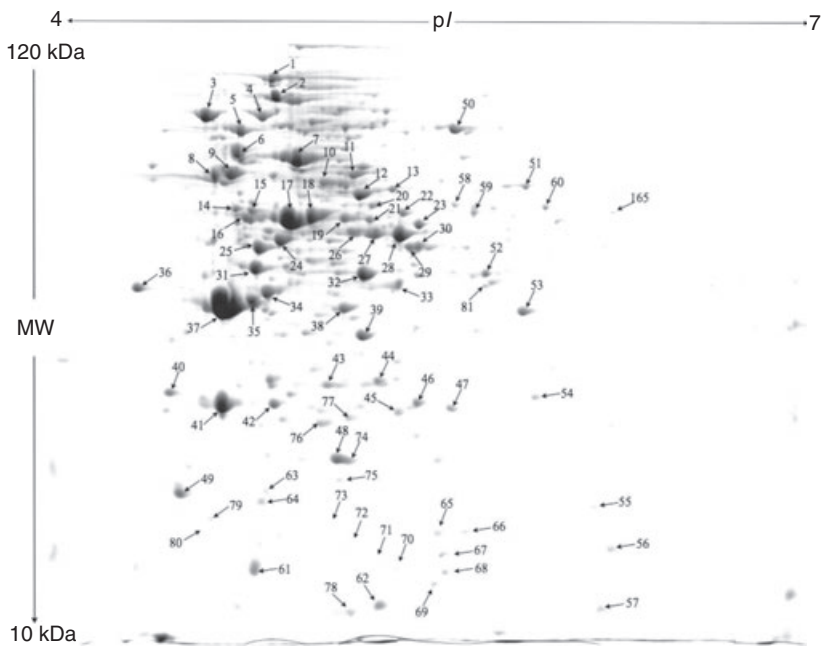

Figure 2 Reference map of *Vibrio tapetis* CECT 4600^T. The identified proteins are labelled with spot numbers (from 1 to 81 and 165) and listed in Table 1.

www.ncbi.nlm.nih.gov/COG/old/). Most of the identified proteins were involved in 'cellular processes' and 'metabolism' classes (85% of all identified proteins). Proteins involved in 'information, storage and processing' were also identified, and only three proteins were poorly characterized (Fig. 3). More than a half (66%) of the proteins belonging to the cellular processes and metabolism classes could be grouped within four of the 13 possible COG functional categories as follows: (i) 'carbohydrate transport and metabolism' (G), (ii) 'post-translational modification, protein turnover and chaperones' (O), (iii) 'energy production' (C) and (iv) 'amino acid transport and metabolism' (E). The rest of the identified proteins were related with other COG categories, including 'inorganic ion transport and metabolism' (P); 'cell envelope biogenesis and outer membrane' (M); 'signal transduction mechanism' (T); 'translation, ribosomal structure and biogenesis' (J); 'transcription' (K); 'DNA replication, recombination and repair' (L); 'lipid metabolism' (I); and 'coenzyme metabolism' (H) and 'nucleotide transport and metabolism' (F) (Fig. 3).

The 20 most abundant proteins are listed in Table 3. Among these proteins, 40% were involved in 'cellular processes', 35% in 'metabolism', 20% in 'information,

Table 1 Proteins in the proteome of *Vibrio tapetis* CECT 4600^T identified using mass spectrometry

COG category	Protein	Spot	pI*	Strain†
Metabolism				
Carbohydrate transport and metabolism	Fructose-1,6-bisphosphatase	52, 149	5·6, 5·6	A/B
	Glucose-specific PTS system enzyme IIA component	49, 131	4·5, 4·5	A/B
	Aconitate hydratase	1, 82	4·9, 4·9	A/B
	Isocitrate dehydrogenase, NADP-dependent	4, 84	4·9, 4·9	A/B
	Succinyl-CoA synthetase	24, 39, 98, 99, 109	4·9, 5·2, 4·8, 4·9, 5·2	A/B
	Succinate dehydrogenase iron–sulphur protein	43, 46 116, 123	5·1, 5·3 5·1, 5·3	A/B
	Succinate dehydrogenase flavoprotein subunit	50, 152	5·5, 5·5	A/B
	Dihydrolipoamide dehydrogenase	51, 153	5·8, 5·7	A/B
	Enolase	18, 95	5·0, 5·1	A/B
	Fructose-bisphosphate aldolase	31, 101	4·9, 4·8	A/B
	Transaldolase B	35, 106	4·8, 4·8	A/B
	Glucose-1-phosphate adenylyltransferase	23	5·4	A
	fumarate hydratase	11	5·2	A
	Citrate synthase	59	5·6	A
	Phosphoglycerate kinase	25*	4·9	A
	Glyceraldehyde-3-phosphate dehydrogenase	32	5·2	A
	Triosephosphate isomerase	42	4·9	A
Energy production and conversion	malate dehydrogenase	34, 105	4·9, 4·9	A/B
	Phosphoenolpyruvate carboxykinase	7, 86, 87	5·0, 4·9, 5·0	A/B
	F0F1 ATP synthase subunit beta	9, 90	4·7, 4·7	A/B
	ATPase	12, 94	5·2, 5·2	A/B
	Glycerol kinase	10	5·1	A
	Acetate kinase	21	5·2	A
	deoxyribose-phosphate aldolase	113	4·9	B
	Isocitrate dehydrogenase, NADP dependent	84	4·9	B
Amino acid transport and metabolism	serine hydroxymethyltransferase	22, 165, 163	5·3, 6·2, 6·1	A/B
	Alanine dehydrogenase	26, 28, 151	5·2, 5·3, 5·3	A/B
	Acetylornithine aminotransferase	29, 15	5·3, 4·9	A/B
	Amino acid ABC transporter protein	53, 146, 148, 159	5·8, 6·0, 5·7, 6·7	A/B
	Aminopeptidase B	60, 154	5·8, 5·8	A/B
	Diaminopimelate decarboxylase	16	4·9	A
	Cysteine synthase A	33	5·3	A
	Ketol-acid reductoisomerase	8	4·6	A
	Aspartate aminotransferase	30	5·4	A
	Lysine/arginine/ornithine transporter subunit	147	5·8	B
Nucleotide transport and metabolism	Uridine phosphorylase	44, 117	5·2, 5·2	A/B
	Purine nucleoside phosphorylase	76, 122	5·1, 5·0	A/B
	Adenylosuccinate synthetase	13	5·3	A
	Nucleoside diphosphate kinase	70	5·3	A
	UDP-glucose/GDP mannose dehydrogenase	93	5·1	B
	Adenylate kinase	114	4·9	B
Lipid metabolism	3-hydroxydecanoyl-ACP dehydratase	65, 139	5·4, 5·4	A/B
Coenzyme metabolism	6,7-dimethyl-8-ribityllumazine synthase	68	5·5	A
	Uroporphyrogen decarboxylase	164	5·8	B
Cellular Processes				
Post-translational modification, protein turnover, chaperones	Molecular chaperone DnaK	3, 85	4·9, 4·9	A/B
	Heat shock protein 60 family chaperone GroEL	6, 89	4·8, 4·8	A/B
	Peptidyl-prolyl cis-trans isomerase	40, 120, 128	4·5, 4·5, 4·8	A/B
	Alkyl hydroxyperoxide C22 protein	41, 118, 119	4·6, 4·8, 4·6	A/B
	ATP-dependent Clp protease, subunit ClpP	74, 134	5·1, 5·1	A/B
	DNA-binding H-NS	78, 136	5·1, 5·1	A/B
	Stringent starvation protein A	77	5·1	A
	stress-induced protein UspE	81	5·6	A

Table 1 (*Continued*)

COG category	Protein	Spot	pI*	Strain†
Signal transduction mechanisms	dnaK suppressor protein	73, 135	5·1, 5·1	A/B
	S-ribosylhomocysteinase	74	5·1	A
	Stress-induced protein UspE	81	5·6	A
	cAMP regulatory protein	160	6·8	A
Inorganic ion transport and metabolism	Superoxide dismutase [Fe]	48, 133	5·1, 5·1	A/B
	TRAP transporter solute receptor TAXI family precursor	157, 158	6·7, 6·8	A
	Exopolyphosphatase-like protein	110	5·0	B
Cell envelope biogenesis, outer membrane	Outer membrane protein TolC	15, 97	4·9, 4·8	A/B
Cell division and chromosome partitions	Chromosome segregation ATPase	124	5·4	B
Information storage and processing				
Translation, ribosomal structure and biogenesis	Elongation factor G	2, 83	4·9, 4·9	A/B
	Elongation factor Tu	17, 125	4·9, 4·8	A/B
	50S ribosomal protein L10	56, 62, 137, 144	6·1, 5·2, 5·2, 6·0	A/B
	30S ribosomal protein S1p	5, 57, 88, 143	4·8, 6·0, 4·8, 6·0	A/B
	Translation elongation factor Ts	38, 108	5·1, 5·1	A
	Ribosome recycling factor	58	5·5	A
	Elongation factor P	121	4·5	B
	Tryptophanyl-tRNA synthetase	155	6·4	B
	Tyrosyl-tRNA synthetase	162	6·0	B
Transcription	RNA polymerase alpha-subunit	25*, 100	4·9, 4·8	A/B
	Transcription elongation factor GreA	79	4·6	A
DNA replication, recombination and repair	Holiday junction resolvase-like protein	27	5·2	A
Poorly characterized				
General function prediction only	Haemolysin co-regulated protein Hcp-3	61	4·8	A
	isopenicillin N synthase	11	5·0	B
Function unknown	Hypothetical protein pVT1_26	66, 140	5·6, 5·6	A/B
	Hypothetical protein VSWAT3	45, 91	5·3, 4·7	A/B
	Hypothetical protein VSAK1_11258	72	5·1	A
	Hypothetical protein 1103602000595_AND4_07664	55	6·0	A
	Putative type VI secretion protein VasQ-1	126	4·8	B
	Hypothetical protein MED222	92, 129	4·8, 4·6	B
	UPF0065 protein in clcb–clcd intergenic region	156	6·4	B

Two proteins were identified in this spot.

*Estimated pI of the protein based on their position in the gel.

†A/B, protein was identified in both strains; A, protein was identified in CECT4600^T strain; B, protein was identified in GR0202RD strain.

storage and processing', and 5% were not identified. In terms of COG functional categories, categories C (six proteins) G (four proteins) and O (four proteins) were the most represented.

The most abundant proteins in the COG functional category C (energy production and conversion) were phosphoenolpyruvate carboxykinase, malate dehydrogenase and ATPase synthetase enzyme, which was detected in two different spots being one of them the beta-subunit. The alpha- and beta-subunits of succinyl-CoA synthetase were also identified. COG category G (carbohydrate transport and metabolism) was represented by four proteins involved in the glycolysis/gluconeogenesis pathway: glyceraldehyde-3-phosphate dehydrogenase, enolase, fructose-bisphosphate aldolase and phosphoglycerate kinase. In the COG category O (post-translational modification, protein turnover and chaperones) were included the molecular chaperones Dnak and GroEL (hsp60 family), alkyl hydroperoxide reductase and peptidyl-prolyl cis-trans isomerase B.

However, the second most abundant protein in the gels belonged to the COG category 'translation, ribosomal structure and biogenesis' (J). It was identified as the elongation factor Tu, which is an essential protein for protein synthesis.

The proteome of *V. tapetis* strain GR0202RD was also analysed under the same conditions. Fifty-six spots with similar position in both strains were detected. All these proteins were subjected to MS to assess their identity. In addition, another 27 proteins were subjected to MS to obtain more information about the proteome of strain

Table 2 Proteins in the proteomes of *Vibrio tapetis* CECT 4600^T and GR0202RD identified using *de novo* sequencing

Spot	Protein
14	Conserved hypothetical protein (*Vibrio parahaemolyticus*)
15	Type I secretion outer membrane protein TolC (*Vibrio harveyi*)
20	Beta-lactamase/Glucose-6-phosphate dehydrogenase (*Shewanella halifaxiensis/Streptococcus pneumoniae*)
26	No identification
37	Porin-like protein H (OmpH) (*Vibrio shilonii*)
54	No identification
55	hypothetical protein V12G01_08700 (*Vibrio alginolyticus*)
64	Glycine cleavage system regulatory protein (*V. parahaemolyticus*)
67	Hypothetical protein VCG_002854 (*Vibrio cholerae*)
69	Transcript regulator TetR family (*V. parahaemolyticus*)
71	No identification
80	No identification
96	Elongation factor Tu (*Vibrio splendidus*)
104	Porin-like protein H (OmpH) (*V. shilonii*)

GR0202RD (Fig. 4). From all 56 possible similar proteins, 45 (80%) matched in both position and identity, and only three proteins that matched in position had a different identity (Table 4). For the rest of the proteins, this analysis could not be performed as one or both proteins of the pairs were not identified using MS (Table 4).

Of the 20 most abundant proteins in the type strain CECT 4600^T (Table 3), 18 were also identified in GR0202RD strain (with the exception of spots 27 and 32). On the other hand, new proteins identified in GR0202RD were classified into COG functional categories. Although GR0202RD strain did not contribute with any new protein in the most represented COG category (carbohydrate transport and metabolism), a new COG category, 'cell division and chromosome partitions' (D), was observed with the identification of the chromosome segregation ATPase.

The most abundant protein in each strain (corresponding to spots 37 and 104) could not be identified by conventional MS or MS/MS. Although in different position in the gels, both spots were identified as the porin-like protein H (OmpH) by *de novo* sequencing.

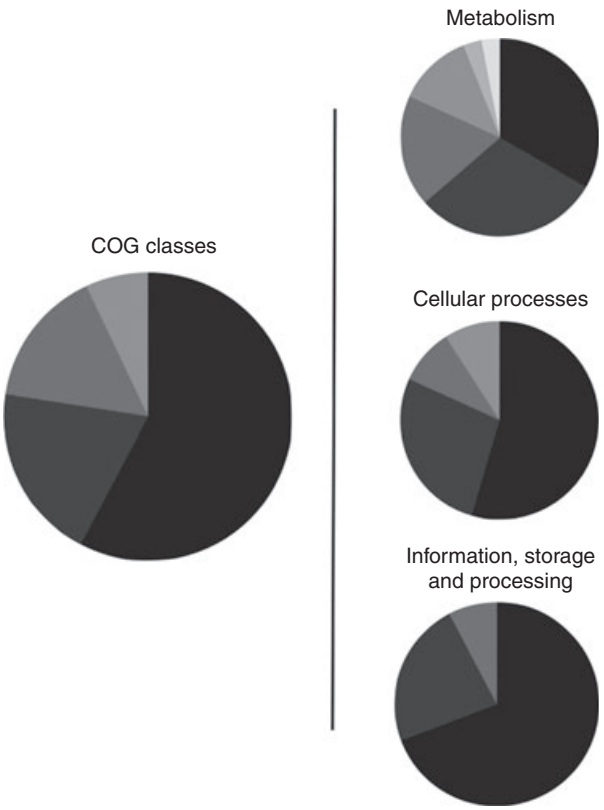

Figure 3 Functional categories of the citoplasmic proteins of *Vibrio tapetis* CECT 4600^T. COG classes: ■ , metabolism; ■, cellular processes; ■, information, storage and processing; ■, poorly characterized. Metabolism: ■, carbohydrate transport and metabolism; ■, amino acid transport and metabolism; ■, energy production and conversion; ■, nucleotide transport and metabolism; ■, lipid metabolism; ■, coenzyme metabolism. Cellular processes: ■, posttranslational modification, proteins turnover, chaperones; ■, singal transduction; ■, inorganic ion transport and metabolism; ■, cell envelope biogenesis, outer membrane. Information, storage and processing: ■, translation, ribosomal structure and biogenesis; ■, transcription; ■, DNA replication, recombination and repair.

Discussion

Vibrio tapetis is an opportunistic pathogen, which has caused important lost in the clam culture all over the world (Paillard 2004). The development of BRD is the result of complex interactions between the pathogen, its host and the environment and; in fact, *V. tapetis* has been proposed as a model to study the host–pathogen interactions (Paillard 2011). As the complete genome of this micro-organism, although under preparation (C. Paillard, personal communication), is not yet published, the proteomic approach may help to clarify its interactions with the clam and the disease processes. In this work, the proteome reference map of *V. tapetis* is described under laboratory conditions using two strains of the species with remarkable differences at genetic and pathophysiological levels (Borrego *et al.* 1996; Novoa *et al.* 1998; Rodríguez *et al.* 2006).

A high reproducibility was obtained for the protein profiles of the *V. tapetis* strains, the majority of the spots being detected in the acidic part of the 2D gels. This finding is in agreement with results of other authors observing a predominance of proteins with low p*I* over high p*I* in halophilic bacteria (Kiraga *et al.* 2007).

Table 3 Twenty most abundant proteins in the *Vibrio tapetis* CECT4600^T 2-DE reference map

Protein*	Spot No†	COG category‡
Unknown protein	37	Function unknown
Elongation factor Tu	17	Translation, ribosomal structure and biogenesis
Alkyl hydroperoxide reductase	41	Post-translational modification, protein turnover, chaperones
Phosphoenolpyruvate carboxykinase	7	Energy production and conversion
Alanine dehydrogenase	28	Amino acid transport and metabolism
Glyceraldehyde-3-phosphate dehydrogenase	32	Carbohydrate transport and metabolism
Enolase	18	Carbohydrate transport and metabolism
Molecular chaperone DnaK	3	Post-translational modification, protein turnover, chaperones
Fructose-bisphosphate aldolase	31	Carbohydrate transport and metabolism
F0F1 ATP synthase subunit beta	9	Energy production and conversion
Heat shock protein 60 family chaperone GroEL	6	Post-translational modification, protein turnover, chaperones
Malate dehydrogenase	34	Energy production and conversion
Phosphoglycerate kinase/RNA polymerase alpha-subunit	25	Carbohydrate transport and metabolism/transcription
ATPase	12	Energy production and conversion
Succinyl-CoA synthetase Subunit beta	24	Energy production and conversion
Succinyl-CoA synthetase subunit alpha	39	Energy production and conversion
Holliday junction resolvase-like protein [*Vibrio* sp.]	27	Low score; *de novo* sequencing.
Elongation factor G	2	Translation, ribosomal structure and biogenesis
Translation elongation factor Ts	38	Translation, ribosomal structure and biogenesis
Peptidyl-prolyl cis-trans isomerase B	61	Post-translational modification, protein turnover, chaperones

*Proteins are listed from most abundant to less abundant according to their expression.
†Spot number from Fig. 2.
‡COG categories according to http://www.ncbi.nlm.nih.gov/COG/old/palox.cgi?fun=all

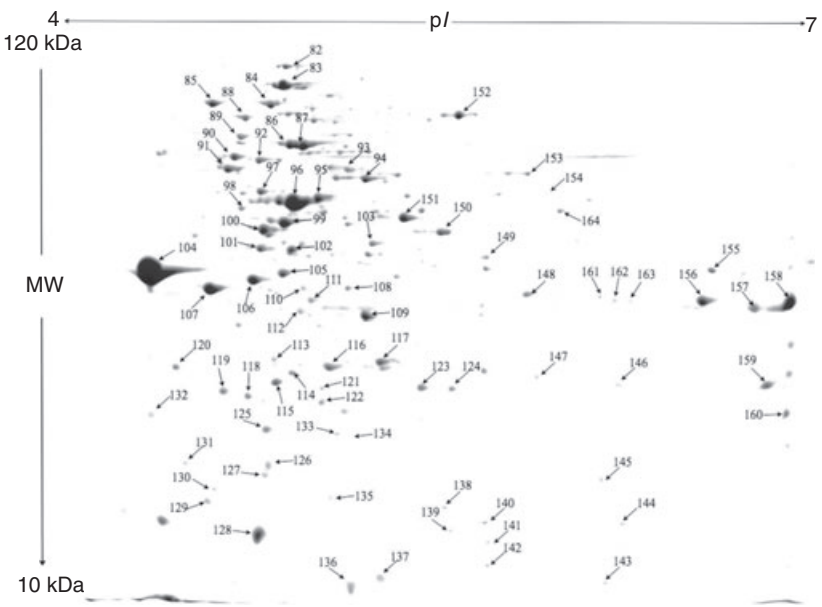

Figure 4 Reference map of *Vibrio tapetis* GR0202RD. The identified proteins are labelled with spot numbers (from 82 to 164) and listed in Table 1.

Similar to other bacterial proteomes (Coelho *et al.* 2004; Chung *et al.* 2007), most of the identified proteins were involved in 'cellular processes' and 'metabolism' classes and in a lesser extent in 'information, storage and processing' class. The most represented COG functional categories were 'carbohydrate transport and metabolism' (G); 'post-translational modification, protein turnover and chaperones' (O); 'energy production' (C); and 'amino acid transport and metabolism' (E). These results are logically expected because within these categories, there are very important pathways, which are essential for the cell survival.

Table 4 Relation between proteins with matched position and their identification using MS

Spot matched in position		Same identification by MS	Spot matched in position		Same identification by MS
CECT 4600^T	GR0202RD		CECT 4600^T	GR0202RD	
1	82	Yes	47	124	Yes
2	83	Yes	48	133	Yes
3	85	Yes	49	131	Yes
4	84	Yes	50	152	Yes
5	88	Yes	51	153	Yes
6	89	Yes	52	149	Yes
7	87	Yes	53	148	Yes
8	91	Yes	54	146	No
9	90	Yes	55	146	No
12	94	Yes	56	144	Yes
15	97	Yes	57	143	Yes
17	96	Yes	60	154	Yes
18	95	Yes	61	128	Yes
24	99	Yes	62	137	Yes
25	100	Yes	63	126	No
28	151	Yes	64	127	No
29	150	Yes	65	139	Yes
31	101	Yes	66	140	Yes
34	105	Yes	67	141	No
35	106	Yes	68	148	No
38	108	Yes	73	135	Yes
39	109	Yes	74	134	Yes
40	120	Yes	76	122	Yes
41	119	Yes	78	136	Yes
43	116	Yes	79	130	No
44	117	Yes	80	129	No
46	123	Yes			

The most abundant detected protein was phosphoenolpyruvate carboxykinase which, although is related to COG category 'energy production and conversion', has also a main role in the gluconeogensis, which is related to the COG 'carbohydrate transport and metabolism' pathway. Phosphoenolpyruvate carboxykinase converts oxalacetate into phosphoenolpyruvate and carbon dioxide and plays an important role in the reversion of the irreversible reaction of pyruvate kinase (Hanson and Patel 1994). The second most abundant protein is the elongation factor Tu, which is an essential protein for protein synthesis. Alkyl hydroperoxide reductase was the third most abundant protein, but its high expression was unexpected because it takes part in the oxidative defence system of the cell in situations with high levels of H_2O_2 (VanBogelen *et al.* 1987).

Malate dehydrogenase was also identified in the 2D gels. This enzyme is involved in the TCA cycle, but also in the gluconeogenesis as it catalyses the conversion of malate into oxalacetate (Gietl 1992). It is noteworthy the finding into the top 20 most abundant proteins of two enzymes that are linked together. Thus, the product of the reaction catalysed by one enzyme serves as substrate for the second enzyme. In this case, oxalacetate, the product of malate dehydrogenase reaction, serves as substrate for the reaction catalysed by phosphoenolpyruvate carboxykinase in the gluconeogenesis pathway.

ATPase synthetase enzyme, detected in two different spots, is the major producer of ATP in bacterial cells. One of these identifications was the beta-subunit of ATP synthetase, which is important as a main component of the second stalk connecting the F1 and F0 sectors, being essential for normal assembly and function (Dunn *et al.* 2000). The detected alpha- and beta-subunits of succinyl-CoA synthetase play a role in the formation of succinate and coenzyme-A from succinyl-CoA in a reversible reaction in the TCA cycle. In addition, this reaction generates one molecule of GTP, which transfers the phosphate group to ADP to generate one ATP (32). On the other hand, high expression of peptidyl-prolyl cis-trans isomerase B, Dnak and GroEL was not surprising as they are essential for protein folding in the cell (Hayano *et al.* 1991; Gragerov *et al.* 1992).

For comparative purposes, the proteome of strain GR0202RD was also characterized. This strain shows different serological properties than CECT 4600^T strains as evidenced by slide agglutination and dot-blot assays (Novoa *et al.* 1998; López *et al.* 2011). In addition, they belong to different genogroups within *V. tapetis* as demonstrated employing several PCR typing methods and ribotyping (Romalde *et al.* 2002; Rodríguez *et al.* 2006). On the other hand, both strains have shown different degree of virulence and host specificity (Novoa *et al.* 1998; Allam *et al.* 2002). For the 56 possible similar proteins between both strains, confirmation of identity was obtained in 80% of the selected spots, and only three proteins that matched in position had a different identity. The 20 most abundant proteins were the same between both *V. tapetis* strains, confirming that these proteins either not change in their amino acid sequence between these strains or present only minor changes that do not alter the pI of the protein. This finding suggests that these abundant proteins are important for the proper performance and survival of any strain of *V. tapetis*.

It is interesting to point out that the most abundant protein in both strains rendered no positive match by MS or MS/MS, although by *de novo* sequencing, it could be identified as porin-like protein H (OmpH). This finding confirms that both strains present the same most abundant protein, even though showing slight changes in the amino acid sequence that causes an alteration in the mobility of the protein at pI but not at molecular weight level. This protein is one of the major outer membrane proteins and is present in very high copy numbers in the bacterial surface (Lee *et al.* 2006).

On the basis of the identification results, it seems clear that, under the culture conditions employed in this study, glucose degradation is one of the major pathways for energy production, this hypothesis is supported by the fact that four enzymes, involved in four of the ten steps of glycolysis, are among the 20 most abundant identified proteins. In addition, the presence of elongation factors within these most abundant proteins indicates that *V. tapetis* synthesizes and processes a great amount of proteins under the laboratory conditions employed.

The reference map obtained in this study not only demonstrates the similarity under laboratory conditions of two strains of the species with remarkable differences at genetic and pathophysiological levels, but also could constitute the first basic step for a further determination of important proteins and pathways involved in the virulence of *V. tapetis*.

Acknowledgements

This work was supported in part by grants AGL2006-13208-C02-01 and AGL2010-18438 from the Ministerio de Ciencia y Tecnología (Spain). J.B.C. and S.B. acknowledge the Xunta de Galicia and the Ministerio de Ciencia e Innovación (MICINN) (Spain) for research fellowships.

References

Allam, B. and Ford, S.E. (2006) Effects of the pathogenic *Vibrio tapetis* on defence factors of susceptible and non-susceptible bivalve species. I. Haemocyte changes following in vitro challenge. *Fish Shellfish Immunol* **20**, 374–383.

Allam, B., Ashton-Alcox, K. and Ford, S.E. (2001) Hemocyte activities associated with resistance to brown ring disease in *Ruditapes* spp. clams. *Dev Comp Immunol* **25**, 365–375.

Allam, B., Paillard, C. and Ford, S.E. (2002) Pathogenicity of *Vibrio tapetis*, the etiological agent of brown ring disease (BRD) in clams. *Dis Aquat Org* **48**, 221–231.

Altschul, S.F., Madden, T.L., Schäffer, A.A., Zhang, J., Zhang, Z., Miller, W. and Lipman, D.J. (1997) Gapped BLAST and PSI-BLAST: a new generation of protein database search programs. *Nucleic Acids Res* **25**, 3389–3402.

Borrego, J.J., Castro, D., Luque, A., Paillard, C., Maes, P., García, M.T. and Ventosa, A. (1996) *Vibrio tapetis* sp. nov., the causative agent of the brown ring disease affecting cultured clams. *Int J Syst Bacteriol* **46**, 480–484.

Bumann, D. (2010) Pathogen proteomes during infection: a basis for infection research and novel control strategies. *J. Proteomics* **73**, 2267–2276.

Cash, P. (2009) Proteomics in the study of the molecular taxonomy and epidemiology of bacterial pathogens. *Electrophoresis* **30**, 133–141.

Cash, P. and Argo, E. (2009) Analysis of bacterial proteins by 2DE. *Methods Mol Biol* **519**, 131–144.

Castro, D., Santamaria, J.A., Luque, A., Martínez-Manzanares, E. and Borrego, J.J. (1996) Antigenic characterization of the etiological agent of the brown ring disease affecting Manila clams. *System Appl Microbiol* **19**, 231–239.

Castro, D., Santamaría, J.A., Luque, A., Martínez-Manzanares, E. and Borrego, J.J. (1997) Determination of the etiological agent of brown ring disease in southwestern Spain. *Dis Aquat Org* **29**, 181–188.

Choquet, G. (2004) Pathogénie de *Vibrio tapetis*, bacteria responsible de la maladie de lánneau brun chez la palourde: approche cellulaire et moléculaire. PhD thesis. University of Brest, Brest.

Choquet, G., Soudant, P., Lambert, C., Nicolas, J.L. and Paillard, C. (2003) Reduction of adhesion properties on *Ruditapes philippinarum* hemocytes exposed to *Vibrio tapetis*. *Dis Aquat Org* **57**, 109–116.

Chung, W.J., Shu, H.Y., Lu, C.Y., Wu, C.Y., Tseng, Y.H., Tsai, S.F. and Lin, C.H. (2007) Qualitative and comparative proteomic analysis of *Xanthomonas campestris* pv. *campestris* 17. *Proteomics* **7**, 2047–2058.

Coelho, A., de Oliveira Santos, E., Faria, M.L., de Carvalho, D.P., Soares, M.R., von Kruger, V.M. and Bisch, P.M. (2004) A proteome reference map for *Vibrio cholerae* El Tor. *Proteomics* **4**, 1491–1504.

De La Fuente, M., Borrajo, A., Bermúdez, J., Lores, M., Alonso, J., López, M., Santalla, M., De Ron, A.M. *et al.* (2011) 2-DE-based proteomic analysis of common bean (*Phaseolus vulgaris* L.) seeds. *J. Proteomics* **74**, 262–267.

Dunn, S.D., Revington, M., Cipriano, D.J. and Shilton, B.H. (2000) The b subunit of *Escherichia coli* ATP synthase. *J Bioenerg Biomembr* **32**, 347–355.

Gietl, C. (1992) Malate dehydrogenase isoenzymes: cellular locations and role in the flow of metabolites between the cytoplasm and cell organelles. *Biochim Biophys Acta* **1100**, 217–234.

Görg, A., Postel, W. and Günther, S. (1988) The current state of two-dimensional electrophoresis with immobilized pH gradients. *Electrophoresis* **9**, 531–546.

Gragerov, A., Nudler, E., Komissarova, N., Gaitanaris, G.A., Gottesman, M.E. and Nikiforov, V. (1992) Cooperation of GroEL/GroES and DnaK/DnaJ heat shock proteins in preventing protein misfolding in *Escherichia coli*. *Proc Natl Acad Sci USA* **89**, 10341–10344.

Hanson, R.W. and Patel, Y.M. (1994) Phosphoenolpyruvate carboxykinase (GTP): the gene and the enzyme. *Adv Enzymol Relat Areas Mol Biol* **69**, 203–281.

Hayano, T., Takahashi, N., Kato, S., Maki, N. and Suzuki, M. (1991) Two distinct forms of peptidylprolyl-cis-trans-isomerase are expressed separately in periplasmic and cytoplasmic compartments of *Escherichia coli* cells. *Biochemistry* **30**, 3041–3048.

Jones, T.H., Johns, M.W. and Gill, C.O. (2008) Changes in the proteome of *Escherichia coli* during growth at 15°C after

incubation at 2, 6 or 8°C for 4 days. *Int J Food Microbiol* **124**, 299–302.

Kan, B., Habibi, H., Schmid, M., Liang, W., Wang, R., Wang, D. and Jungblut, P.R. (2004) Proteome comparison of *Vibrio cholerae* cultured in aerobic and anaerobic conditions. *Proteomics* **4**, 3061–3067.

Kiraga, J., Mackiewicz, P., Mackiewicz, D., Kowalczuk, M., Biecek, P., Polak, N., Smolarczyk, K., Dudek, M.R. *et al.* (2007) The relationships between the isoelectric point and: length of proteins, taxonomy and ecology of organisms. *BMC Genomics* **8**, 163.

von Krüger, W.M., Lery, L.M., Soares, M.R., de Neves-Manta, F.S., Batista e Silva, C.M., Neves-Ferreira, A.G., Perales, J. and Bisch, P.M. (2006) The phosphate-starvation response in *Vibrio cholerae* O1 and phoB mutant under proteomic analysis: disclosing functions involved in adaptation, survival and virulence. *Proteomics* **6**, 1495–1511.

Laemmli, U.K. (1970) Cleavage of structural proteins during the assembly of the head of bacteriophage T4. *Nature* **227**, 680–685.

Lakhal, F., Bury-Moné, S., Nomane, Y., Le Goïc, N.L., Paillard, C. and Jacq, A. (2008) DjlA, a membrane-anchored DnaJ-like protein, is required for cytotoxicity of clam pathogen *Vibrio tapetis* to hemocytes. *Appl Environ Microbiol* **74**, 5750–5758.

Lane, E. and Birkbeck, T.H. (2000) Species specificity of some bacterial pathogens of bivalve molluscs is correlated with their interaction with bivalve haemocytes. *J Fish Dis* **23**, 275–279.

Le Chevalier, P., Boula, C. and Paillard, C. (2003) Characterization by restriction fragment length polymorphism and plasmid profiling of *Vibrio tapetis* strains. *J Basic Microbiol* **5**, 414–422.

Lee, A.Y., Park, S.G., Jang, M., Cho, S., Myung, P.K., Kim, Y.R., Rhee, J.H., Lee, D.H. *et al.* (2006) Proteomic analysis of pathogenic bacterium *Vibrio vulnificus*. *Proteomics* **6**, 1283–1289.

López, J.R., Balboa, S., Núñez, S., de la Roca, E., de la Herran, R., Navas, J.I., Toranzo, A.E. and Romalde, J.L. (2011) Characterization of *Vibrio tapetis* strains isolated from diseased cultured Wedge sole (*Dicologoglossa cuneata* Moreau). *Res Vet Sci* **90**, 189–195.

López-Cortés, L., Luque, A., Martínez-Manzanares, E., Castro, D. and Borrego, J.J. (1999) Adhesion of *Vibrio tapetis* to clam cells. *J Shellfish Res* **18**, 91–97.

Neuhoff, V., Arold, N., Taube, D. and Ehrhardt, W. (1988) Improved staining of proteins in polyacrylamide gels including isoelectric focusing gels with clear background at nanogram sensitivity using Coomassie Brilliant Blue G-250 and R-250. *Electrophoresis* **9**, 255–262.

Nishimura, J.S. (1986) Succinyl-CoA synthetase structure-function relationships and other considerations. *Adv Enzymol Relat Areas Mol Biol* **58**, 141–172.

Novoa, B., Luque, A., Castro, D., Borrego, J.J. and Figueras, A. (1998) Characterization and infectivity of four bacterial strains isolated from brown ring disease-affected clams. *J Invertebr Pathol* **71**, 34–41.

Osman, K.M., Ali, M.M., Radwan, M.I., Kim, H.K. and Han, J. (2009) Comparative proteomic analysis on *Salmonella gallinarum* and *Salmonella enteridis* exploring proteins that may incorporate host adaptation in poultry. *J. Proteomics* **72**, 815–821.

Paillard, C. (2004) A short-review of brown ring disease, a vibriosis affecting clams, *Ruditapes philippinarum* and *Ruditapes decussatus*. *Aquat Living Resour* **17**, 467–475.

Paillard, C. (2011) Vibriosis comparison between marine organisms models: is there specificity in host-pathogen interactions? In *Vibrio2011.The Fourth Conference on the Biology of Vibrios* ed. Romalde, J.L. 93 pp. Lalín, Spain: Alvarellos SL.

Paillard, C. and Maes, P. (1995) The brown ring disease in the Manila clam, *Ruditapes philippinarum*. I. Ultrastructural alterations of the periostracal lamina. *J Invertebr Pathol* **65**, 91–100.

Paillard, C., Maes, P. and Oubella, R. (1994) Brown ring disease in clams. *Annu Rev Fish Dis* **4**, 219–240.

Phillips, C.I. and Bogyo, M. (2005) Proteomics meets microbiology: technical advances in the global mapping of protein expression and function. *Cell Microbiol* **7**, 1061–1076.

Poobalane, S., Thompson, K.D., Diab, A., Ardó, L., Jeney, G. and Adams, A. (2008) Protein expression by *Aeromonas hydrophila* during growth *in vitro* and *in vivo*. *Microb Pathog* **45**, 60–69.

Rodríguez, J.M., López-Romalde, S., Beaz, R., Alonso, M.C., Castro, D. and Romalde, J.L. (2006) Molecular fingerprinting of *Vibrio tapetis* strains using three PCR-based methods: ERIC-PCR, REP-PCR, and RAPD. *Dis Aquat Org* **69**, 175–183.

Romalde, J.L., Castro, D., Magariños, B., Lopez-Cortes, L. and Borrego, J.J. (2002) Comparison of ribotyping, randomly amplified polymorphic DNA, and pulsed-field gel electrophoresis for molecular typing of *Vibrio tapetis*. *Syst Appl Microbiol* **25**, 544–550.

Roncada, P., Deriu, F., Gaviraghi, A., Martino, P.A. and Bonizzi, L. (2009) Proteomic study of antibiotic resistance in *Escherichia coli* strains. *Vet Res Commun* **33**, 157–160.

Sharma, P., Kumar, B.N., Singhal, V.M., Katoch, K., Venkatesan, D.S., Chauhan, D. and Bisht, D. (2010) Streptomycin induced protein expression analysis in Mycobacterium tuberculosis by two-dimensional gel electrophoresis & mass spectrometry. *Indian J Med Res* **132**, 400–408.

Trinkler, N., Sinquin, G., Querne, J. and Paillard, C. (2010) Resistance of brown ring disease in the Manila clam, *Ruditapes philippinarum*: a study of selected stocks showing a recovery process by shell repair. *J Invertebr Pathol* **104**, 8–16.

Trinkler, N., Guichard, N., Labonne, M., Plasseraud, L., Paillard, C. and Marin, F. (2011) Variability of shell repair in

the Manila clam *Ruditapes philippinarum* affected by the brown ring disease: a microstructural and biochemical study. *J Invert Pathol* **106**, 407–417.

VanBogelen, R.A., Kelley, P.M. and Neidhardt, F.C. (1987) Differential induction of heat shock, SOS, and oxidative stress regulons and accumulation of nucleotides in *Escherichia coli*. *J Bacteriol* **169**, 26–32.

Supporting Information

Additional Supporting Information may be found in the online version of this article:

Table S1 Additional data on MS protein identification. Peptides submitted to MSMS are marked with an asterisk.

Table S2 Results of the identification of proteins by *de novo* sequencing.

Please note: Wiley-Blackwell are not responsible for the content or functionality of any supporting materials supplied by the authors. Any queries (other than missing material) should be directed to the corresponding author for the article.